Noise accelerates synchronization of coupled nonlinear oscillators

David Chik and Adelle Coster
School of Mathematics and Statistics, University of New South Wales, Sydney NSW 2052, Australia
(Received 8 June 2006; revised manuscript received 15 August 2006; published 31 October 2006)

For a chain of homogeneous nonlinear oscillators starting from different initial phases, a certain amount of time is required for the system to evolve to complete phase synchronization. The effect of independent noise in such a system was investigated, and an optimal noise intensity was found that minimized the average synchronization time. Both threshold noise and connection noise show similar effects. The features of the phenomenon and the underlying mechanism are discussed through the analysis of a two-unit system and the numerical studies of chains up to 30 units in length.

DOI: 10.1103/PhysRevE.74.041128 PACS number(s): 05.40.Ca, 05.45.Xt, 87.18.Sn

I. INTRODUCTION

A simple but beautiful phenomenon found in nature is synchrony. Abundant examples such as the flashing of fireflies, the pacemaking of SA node cells, neural firing during the attention state, and the clapping of applauding audiences, have been observed and investigated throughout past decades (two representative books would be [1,2]). Mathematical models have been built aimed at ascertaining the main mechanisms responsible for this behavior. The first successful attempt was the Kuramoto formalism [3,4]. It studied a population of phase oscillators coupled in a global and continuous manner. When each oscillator has a different intrinsic frequency, the system can exhibit a range of collective phenomena including synchrony (where all units are at the same phase) and cluster states (where the units are organized into a few groups of common phases) [5–8]. In the framework of nonlinear dynamics, biological systems such as neurons and heart cells belong to the class of excitable systems, which is characterized by the presence of a threshold. The system will stay in the rest state until the input signal exceeds the threshold, after which the system jumps into a short excited state before returning to the rest state. This dynamics is usually described by the integrate and fire model [9] or phase oscillator model [10]. The form of coupling between the units is, however, local (or regional) and pulsatile, which requires more sophisticated methods to analyze the state of the system [11–13].

Most studies have focused on systems in the absence of noise. However, noise is inevitably present in the real world. Microscopically, for instance, the random switching of membrane ion channels causes the fluctuation of firing times of a cell, and the random formation or destruction of gap junctions or synapses cause fluctuations in connection strength. Macroscopically, physiological signals such as heart rate variability are also found to be extraordinarily complex. Intuitively, the effect of noise seems to blur out the observable patterns. However, interesting phenomena where noise plays a constructive role have also been found (for a review, see [14]). For example, noise may induce synchronization in excitatory neural networks [15,16] and clusters in inhibitory networks [17]. In particular, in the case of a network of sparsely firing neuronal units (due to insufficient current input), the addition of an optimal intensity of noise can encourage more units to fire and also produce a higher degree of coherence for the whole network. This "noise enhances coherence" phenomenon has been observed in Hodgkin-Huxley [18] and Fitz Hugh-Nagumo systems [19]. There also exists another interesting type of noise-induced synchronization for uncoupled systems. In this case the units have different initial phases, but the application of a common noise gradually reduces their phase differences, and eventually brings the system to a stochastic equilibrium [20–22].

Apart from the question about whether synchrony occurs or not, the amount of time taken to achieve the synchronous state is also an important question because biological systems have to be robust against occasional perturbations and be able to return back to the stable pattern rapidly. If a complete phase synchronization is to occur in a network of oscillators, it will take a given time depending on the initial state as well as the connectivity of the network. The time will be shorter if the excitatory coupling is strong [11] and if there are more connections in the network [12]. For a chain of homogeneous spiking oscillators in the absence of noise, the synchronization rate was found to be proportional to $\log(N)$, where N is the number of units [23]. However, the effect of noise on the synchronization rate is unclear. In this paper, we report a scenario that there exists an optimal range of noise intensity for which the synchronizing process is accelerated.

II. MODEL AND METHOD

A. Model

We chose a linear chain of homogeneous oscillators to investigate the role of noise in synchronization timing. This avoids the complications in systems of units with different intrinsic frequencies, which exhibit a wide range of collective behavior including phase locking clusters and waves. We consider a nonleaky integrate-and-fire model with a constant input, which serves as the simplest representative of excitable systems. Let V_i be the potential of unit i,

$$\frac{dV_i}{dt} = 1, \quad i \in [1, \ldots, N]. \tag{1}$$

An action potential (spike) will be produced when it reaches the threshold ($V_i = V_{th} = 1$), after which it will be reset

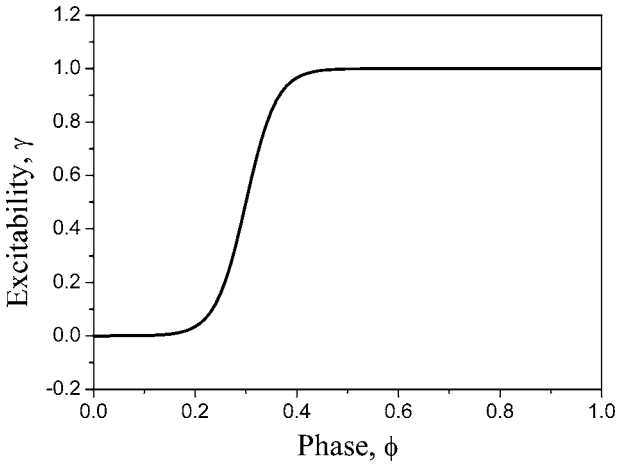

FIG. 1. The refractory function. The vertical axis represents the excitability γ of a unit in our system. The horizontal axis represents the instantaneous phase when the signal arrives. $\alpha=\frac{10}{0.3}$, $\tau=0.3$.

to zero ($V_i=0$). Thus all N units have an identical intrinsic period of one.

Each unit is connected with the two nearest neighbors (left and right), except the units at the two ends (which only have one neighbor). When one of the units fires, a spike will be transmitted to its neighbors (here we assume no delay). The size of the spike is w, which will be referred to as the connection strength (for simplicity assumed to be identical for all units). Many biological systems such as neurons and cardiac cells are refractory after generating an action potential and are not fully responsive to further input for a period of time. To embody this in our units, we chose a sigmoidal function. Thus the resulting change in potential of the recipient unit i due to a spike from unit j at time t_j is

$$\Delta V_{j\to i} = w_{j\to i}\gamma_i(\phi_i)\delta(t-t_j), \tag{2}$$

where t_j is the time when unit j fires a spike, δ is the delta function (1 when $t=t_j$ or 0 otherwise), and

$$\gamma_i(\phi_i) = 1/(1+e^{\alpha(\tau-\phi_i)}) \tag{3}$$

represents the excitability of the unit (Fig. 1), α and τ are parameters controlling the shape of the phase response, and ϕ_i is the instantaneous phase of the unit when the spike arrives. The phase of a unit is the time since the last spike of the unit relative to its intrinsic (unperturbed) cycle. It is a continuous value between 0 and 1. The resulting equation becomes

$$\frac{dV_i}{dt} = 1 + \sum_j \Delta V_{j\to i} \tag{4}$$

where the summation encompasses the left and right neighbors.

Each unit is subject to an independent noise. The sources of noise can be distinguished into two types, intrinsic and extrinsic [25–27]. Intrinsic noise refers to the noise at the neuronal level such as the fluctuation of membrane potential due to the finite number of ion channels. Extrinsic noise refers to the noise at the network level due to, for instance, background activity. The effect of both types of noise will be explored.

1. Threshold noise

This represents an intrinsic noise. The threshold of a unit is subject to a Gaussian noise of zero mean ξ_{th},

$$V_{th} = 1 + \xi_{th}. \tag{5}$$

For computational convenience, we define the noise intensity (variance) η as the width up to three standard deviations away from the mean. For example, $\eta=0.1$ corresponds to the situation when the three standard deviations of the distribution of ξ_{th} is -0.1 and 0.1.

2. Connection noise

This represents an extrinsic source of noise. The connection strength is modified as

$$w \to w + \xi_{co}, \tag{6}$$

where ξ_{co} is again a Gaussian noise of zero mean and variance η, independent to each unit. Here, the threshold of the units is $V_{th}=1$.

B. Implementation

The program code was written in FORTRAN90. The numerical integration was done by using a simple trapezoidal rule with time step$=10^{-5}$. This was accurate because the terms inside the integral were linear, while γ_i was external. To avoid the effect of ordering, the inputs of all units from their neighbors were determined before updating the states of the units. Initial transitional dynamics were avoided by leaving all units uncoupled for 3×10^5 time steps at the beginning of each run, whereupon they were then connected and the time thereafter recorded. To reduce the computational cost, we did not use a continuous stochastic process. The Gaussian noise was implemented in an event-based manner: a random number was picked whenever the unit was reset. This implementation would affect the scaling of the values of the intensity η, but tests using an Ornstein-Uhlenbeck stochastic process [24] showed that the noise implementation method had no significant effect in itself.

By "synchrony" we mean that the units were all at the same phase. Theoretically, this could be defined as $\lim_{t\to\infty}\|\phi_j-\phi_i\|=0$ where all combinations of (i,j) pairs would be taken into account. When noise is present, however, the system will instead evolve to a state where all units are almost synchronized with a very small fluctuation of phase differences. Thus we provide a computationally tractable definition for synchrony:

$$\max|\phi_j-\phi_i| < \epsilon. \tag{7}$$

Synchrony would be assumed to be attained when the maximum phase difference between the earliest phase and the latest phase in the chain was smaller than ϵ. In our simulations, $\epsilon=0.01$. This was chosen in order to meet two criteria: on one hand, it is large enough such that the final state of

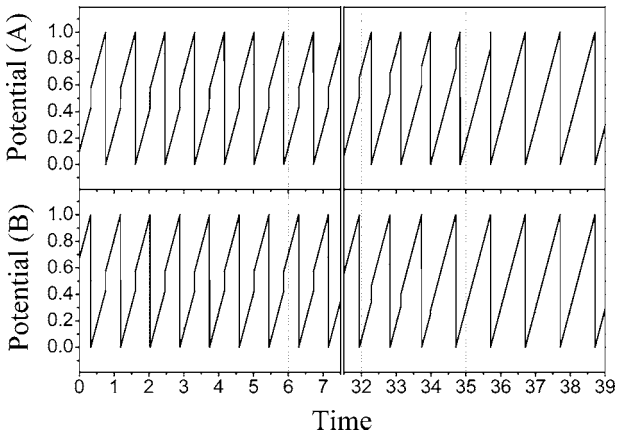

FIG. 2. Traces of the potential of two coupled units (A and B). The coupling strength, w, between the units was set to 0.15. Noise was absent.

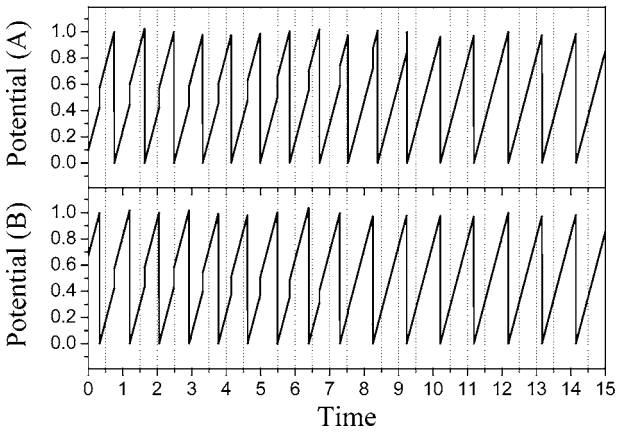

FIG. 3. Effect of noise on the potential traces of two coupled units (A and B). The coupling strength was as Fig. 2. Noise intensity, η, was set to 0.1.

the noisy units will enter and stay in the ϵ window. On the other hand, it is small enough to minimize the possibility of temporary synchronization—a false coherence where the units group up by chance but separate again in the future.

Parameters for the refractory functions were $\alpha=\frac{10}{0.3}$, $\tau=0.3$. Random initial conditions were applied to different oscillators in the chain so that there was no correlation between their initial phases. Without coupling, the oscillators would remain at the same phases and uncorrelated to each other. Notice that in this case the noise is independent to each unit, so the organization effect referred to earlier [20–22] for uncoupled oscillators will not manifest in this system.

III. RESULTS

A. Threshold noise

1. Two units

We begin with an examination of a system of two coupled oscillators in which the connection strengths were $w=0.15$. Figure 2 shows an example set of potentials of the units. Starting from different initial phases and in the absence of noise, the units took around 37 time units to synchronize. However, if a threshold noise of intensity $\eta=0.1$ was applied independently to the same system of two units, they took only ten time units to achieve synchronization, which is shown in Fig. 3. Notice that in this situation the peaks of the potentials fluctuate around the varying threshold $V_{th}=1$.

2. Longer chains

Figure 4 shows an example of firing profile of the chain of $N=30$ units with connection strength $w=0.15$. In the case of no noise, the chain took approximately 16 time units to synchronize [Fig. 4(a)]. Using the same set of initial conditions, when threshold noises of intensity $\eta=0.1$ were applied, the units took approximately 13.5 time units to synchronize [Fig. 4(b)]. For large noise intensity ($\eta=1$), the units fired randomly and never synchronized [Fig. 4(c)].

With the longer chain, internally synchronized clusters of units formed and the system then evolved with a growth of the cluster size until the entire set was synchronized. This is evidenced in Fig. 4. The presence of noise enhanced the formation and merging of the clusters.

The synchronization time is of course dependent on the initial conditions. The histogram in Fig. 5(a) shows the distribution of synchronization times over 100,000 trials of a 30-unit chain with different initial conditions in the absence of noise. For this distribution, the mean value is 42.7 time units, the standard deviation is 29.3 time units, and the standard error is 0.09 time units. In comparison, the histogram for the situation with a noise of $\eta=0.15$ is plotted in Fig. 5(b). In this case, the mean value is 30.9 time units, the standard deviation is 13.1 time units, the standard error is 0.04 time units. The reduction of synchronization times occur as a statistical phenomenon. In the following computations, 3 million trials were performed, ensuring that the standard errors of the average synchronization times were smaller than 0.1 time units in all cases.

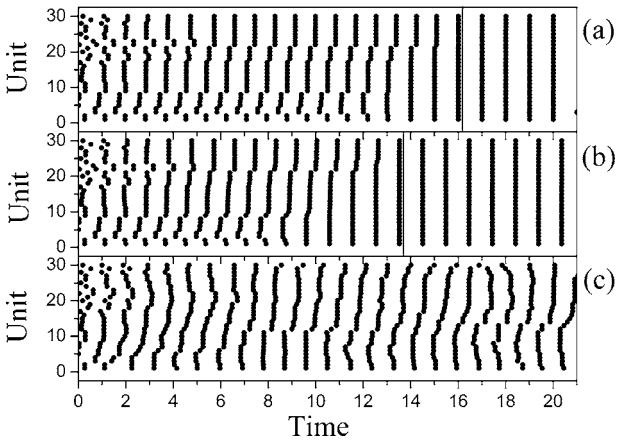

FIG. 4. Effect of noise on the firing profile of 30 units connected as a chain. One black dot corresponds to one spike. The coupling strength was $w=0.15$. Noise intensity (a) $\eta=0$, (b) $\eta=0.1$, and (c) $\eta=1$. The vertical lines indicate the time when the units were approximately synchronized.

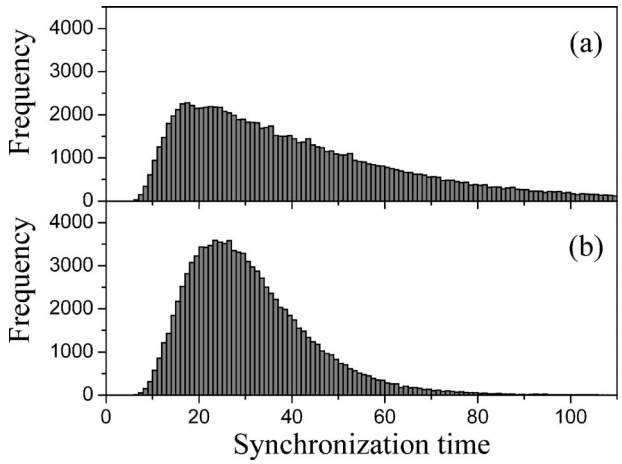

FIG. 5. Histograms of synchronization times from a sample of 100 000 trials of random initial conditions for a 30-unit chain. Connection strength $w=0.1$. Noise intensity (a) $\eta=0$ and (b) $\eta=0.15$.

Figure 6 plots the average synchronization time, S, against noise intensity, η, for various coupling strengths for a 30-unit chain. For weaker connections (e.g., $w=0.1$), S decreased to an optimal level and then increased, forming a J-shaped curve. For stronger couplings (e.g., $w=0.2$), however, the synchronization time appeared to increase monotonically with noise intensity. The curves shifted downwards as connection strength increased.

Figure 7 shows the average synchronization time, S, for $\eta=0$ and η_{opt}, where η_{opt} is the optimal noise intensity, as a function of coupling strength, w, for a 30-unit chain. As expected, S decreased as w increased. In addition, the difference between S at $\eta=0$ and that at $\eta=\eta_{opt}$ diminished as w increased.

To quantify the maximum amount of time reduction due to the effect of noise, we define a reduction ratio Γ:

$$\Gamma = 1 - \frac{\text{synchronization time at optimal } \eta}{\text{synchronization time in the absence of noise}}. \tag{8}$$

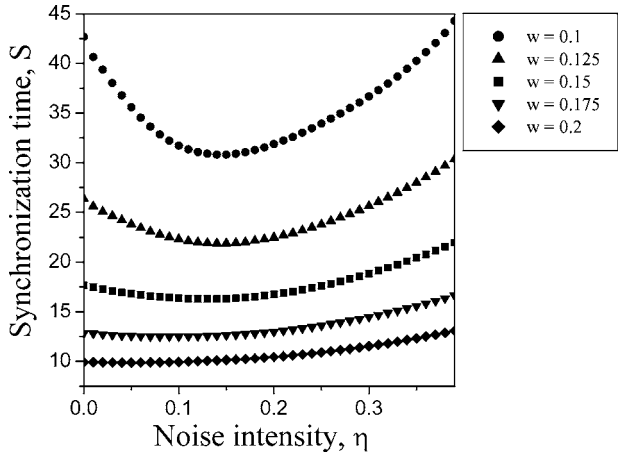

FIG. 6. The average synchronization time S against noise intensity η, for coupling strengths $w=0.1$, 0.125, 0.15, 0.175, and 0.2, for a 30-unit chain. The synchronizing time was averaged from 3 000 000 trials of random initial conditions.

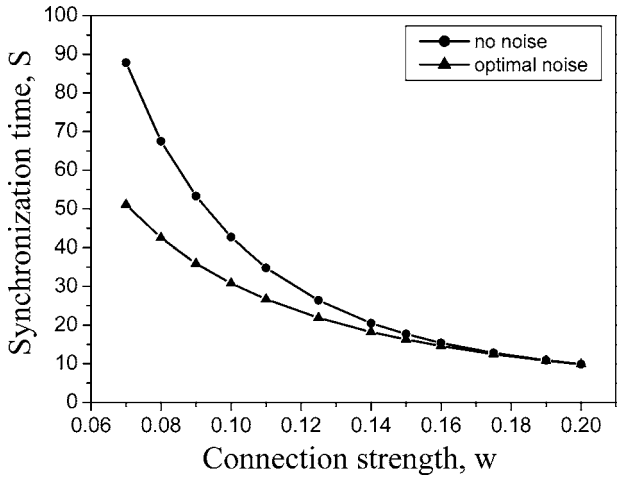

FIG. 7. The average synchronization time S against connection strength w, for no noise ($\eta=0$) and optimum noise levels ($\eta=\eta_{opt}$), for a 30-unit chain.

The maximum reduction ratio Γ as a function of the coupling strength w, for various chain lengths, is shown in Fig. 8. Γ uniformly decreased as w increased, but the curves shifted upward as the chain length increased. In addition, we can identify a weak connection regime from around $w=0.7-0.12$. In this regime, the reduction ratio against connection strength was nearly linear irrespective of chain length. At higher connection strengths, it flattened out towards $\Gamma=0$ at a critical connection strength of approximately $w_c=0.2$.

In Fig. 6, we can also observe that the optimal level of noise, η_{opt}, decreased as the coupling strength increased. It started from around 0.15 and dropped to zero at the same critical connection strength.

B. Connection noise

The average synchronization time S as a function of the connection noise intensity η is shown in Fig. 9. S was again

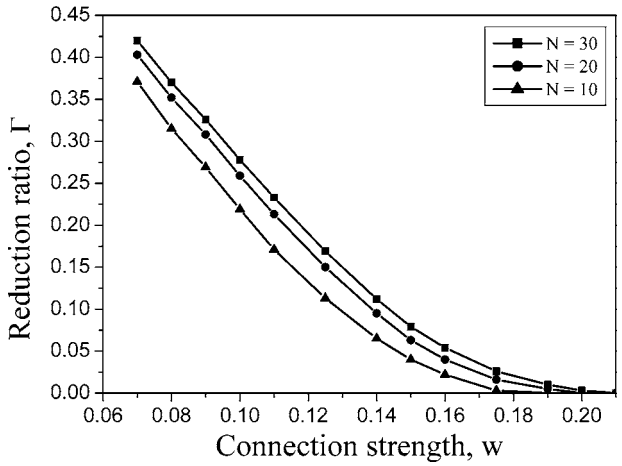

FIG. 8. The reduction ratio Γ of the synchronization times as a function of the coupling strength w, for chain lengths $N=10$, 20, and 30.

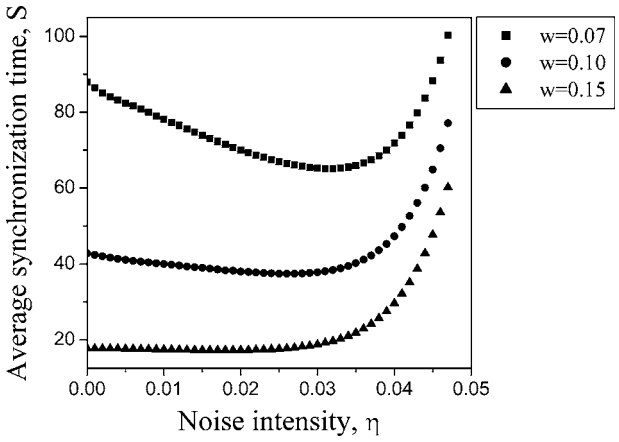

FIG. 9. The average synchronization time S (arbitrary time units) as a function of noise intensity η, for connection strength $w=0.07$, 0.1, and 0.15. The synchronization time was averaged over 3 000 000 trials of random initial conditions. Chain length $N=30$.

averaged over 3 million trial runs. The chain length was $N=30$. The different curves correspond to different connection strengths w. For weaker connections, the synchronization time, similarly to the threshold noise, first decreased and then increased as η increased, forming a J-shaped curve, but it increased monotonically for stronger couplings.

Figure 10 shows the reduction ratio Γ as a function of the coupling strength w. Generally, Γ decreased as w increased, and the curves shifted upward as the chain length N increased. The critical connection strength where $\Gamma \to 0$ was found to be $w_c=0.18$.

C. Comparison

In order to compare between connection noise and threshold noise, in Fig. 11 we show the average synchronization time S vs noise intensity η for the two types of noise, keeping the same connection strength $w=0.1$ and chain length $N=30$ for both cases. The result for threshold noise appeared to be a magnified version of that for connection noise. The

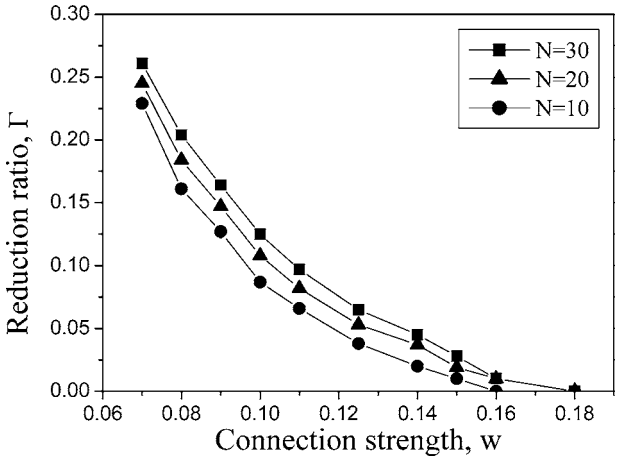

FIG. 10. The reduction ratio Γ as a function of the coupling strength w, for chain lengths $N=10$, 20, and 30.

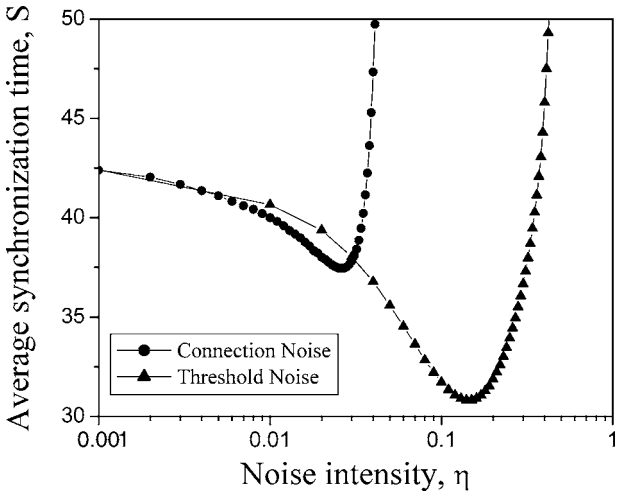

FIG. 11. The average synchronization time S as a function of noise intensity η for connection noise and threshold noise. In both cases, connection strength $w=0.1$, chain length $N=30$.

trend for the case of threshold noise had a deeper valley, and also the minimum was located at a higher value of noise intensity than that for the case of connection noise.

Figure 12 shows the reduction ratio Γ against the coupling strength for the two types of noise, for $N=30$. The trend for the case of threshold noise was found at higher reduction ratios than that of connection noise for all connection strengths up to the critical connection strength ($w_c=0.2$ for the case of threshold noise and $w_c=0.18$ for the case of connection noise).

D. Square lattice (preliminary results)

Simulations were also made on a 10×10 square lattice of units with cyclical boundary conditions. In the chain geometry, the units had two neighbors, whereas in the square lattice each unit has four neighbors. Threshold noise was ap-

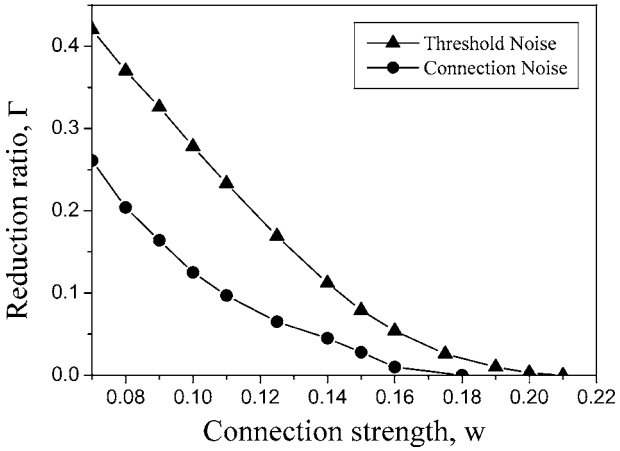

FIG. 12. The reduction ratio Γ as a function of the coupling strength for connection noise and threshold noise. In both cases, chain length $N=30$.

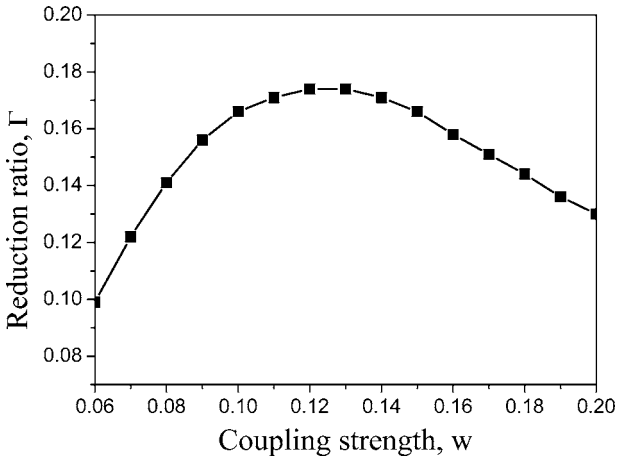

FIG. 13. The reduction ratio Γ as a function of the coupling strength for a 10×10 array of units with cyclical boundary conditions. Threshold noise was applied to the units.

plied to the units. The reduction ratio as a function of connection strength is shown in Fig. 13.

IV. DISCUSSION

A. Threshold noise

1. Two units

In the absence of noise, as shown in Fig. 2, we observe that the phase difference between the two units remained almost unchanged initially and that it took a long time for the system to evolve to total phase synchronization. However, we observe the interesting phenomenon of noise accelerating synchronization (Fig. 3). We may gain some insights about the underlying mechanism by tracing the phases of the two firing units.

When an input is incident to a unit, the time at which the next spike is produced may change. This response depends on the phase (the time relative to the intrinsic cycle of the unit at which the input arrives). This phase is a continuous variable ranging from 0 to 1. There exists a mapping between the voltage and the phase of the unit. The relationship is usually complicated when the voltage grows nonlinearly with time. In our model, however, we deliberately defined the voltage level of each unit to grow piecewise linearly between 0 (reset) and 1 (threshold). This simplification is helpful for analysis and discussion, since a change of potential ΔV is equivalent in quantity to a change of phase of the unit $\Delta\phi$. Thus Eq. (4) can be rewritten in the form of phase oscillators,

$$\frac{d\phi_i}{dt} = 1 + \sum_j \Delta\phi_{j\to i}, \tag{9}$$

where ϕ_i is the phase of the ith oscillator evolving between 0 and 1. The interaction term $\Delta\phi_{j\to i}=\Delta V_{j\to i}=w/(1+e^{\alpha(\tau-\phi_i)})$.

For two such coupled pacemakers A and B, the equations are

$$\frac{d\phi_A}{dt} = 1 + \Delta\phi_{B\to A}(\phi_A), \tag{10}$$

$$\frac{d\phi_B}{dt} = 1 + \Delta\phi_{A\to B}(\phi_B). \tag{11}$$

Suppose at a given time $t=t_0$, unit A is at phase $\phi_A=\phi^{(k)}$ (having emitted k action potentials), and unit B is at phase $\phi_B=0$. The evolution of their phases is shown in Table I, where t_0+t_1 is the time when A next fires, and t_0+t_2 is the time when B next fires. The spike duration is assumed to be very short in time, hence we use $t_0+t_1^+$ and $t_0+t_2^+$ to represent the time directly after the spike. When A fires, the phase of B is altered. Similarly, the firing of B alters the phase of A. Using the phase of B as a reference (Table I), we can calculate the return map for the phase of A due to two consecutive firings of B,

$$\begin{aligned}\phi^{(k+1)} = 1 - [(1-\phi^{(k)}) &+ \Delta\phi_{A\to B}(1-\phi^{(k)})] + \Delta\phi_{B\to A}(1-[(1-\phi^{(k)}) \\ &+ \Delta\phi_{A\to B}(1-\phi^{(k)})]),\end{aligned} \tag{12}$$

$$\phi^{(k+1)} = \phi^{(k)} - \frac{w}{1+e^{\alpha(\tau-1+\phi^{(k)})}} + \frac{w}{1+e^{\alpha(\tau-\phi^{(k)}+w/1+e^{\alpha(\tau-1+\phi^{(k)})})}}. \tag{13}$$

The phase change is defined as

$$\delta\phi = \phi^{(k+1)} - \phi^{(k)} \tag{14}$$

$$= \frac{w}{1+e^{\alpha(\tau-\phi+w/1+e^{\alpha(\tau-1+\phi)})}} - \frac{w}{1+e^{\alpha(\tau-1+\phi)}}, \tag{15}$$

where $\phi=\phi^{(k)}$ for convenience.

There exists an additional restriction on $\delta\phi$ due to the reset mechanism. When the voltage exceeds the threshold, the unit emits an action potential and be reset to zero. This also applies to the phase equations such that any $\phi^{(k+1)}>1$ will be cut off at $\phi^{(k+1)}=1$ and then reset to 0.

Figure 14 shows the curve of the corrected $\delta\phi$ vs ϕ, using parameters $w=0.15$, $\alpha=\frac{10}{0.3}$, and $\tau=0.3$. Notice that there is a zero at around $\phi^*=0.565$. This "lag fixed point" is a repeller because at ϕ^{*-} the value of $\delta\phi$ is negative so that the phase will eventually evolve to 0, and at ϕ^{*+} the value is positive so that the phase will eventually evolve to 1 and be reset to 0. This phase is relative to that of unit B. Thus the two units will finally achieve zero phase difference, although it could take a long time. Indeed in the example shown in Fig. 2, we deliberately set the initial phase difference close to this lag

TABLE I. Phase evolution of two coupled oscillators.

Time	t_0	t_0+t_1	$t_0+t_1^+$	t_0+t_2	$t_0+t_2^+$
Phase of A	$\phi^{(k)}$	1	0	$1-\psi$	$1-\psi+\Delta\phi_{B\to A}(1-\psi)=\phi^{(k+1)}$
Phase of B	0	$1-\phi^{(k)}$	$(1-\phi^{(k)})+\Delta\phi_{A\to B}(1-\phi^{(k)})=\psi$	1	0

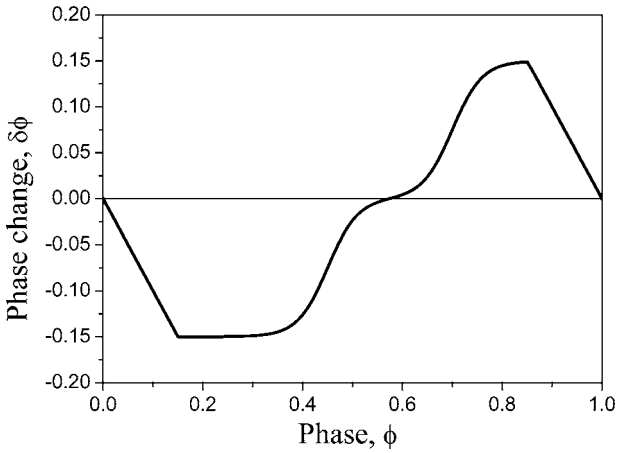

FIG. 14. The phase response in a two-unit system. The vertical axis represents the next phase change after the next firing of the partner unit. The horizontal axis represents the current phase after the current firing of the partner unit. The coupling strength was $w=0.15$.

fixed point, ensuring that the two units took an extended time to synchronize. If the initial phase of the two units is farther away from the lag fixed point, for example, 0.5, then the units will synchronize faster.

The addition of noise to the units will impose an uncertainty on their expected relative phases. If the two units have relative phase close to $\phi=\phi^*$, the noise will help perturb them away from ϕ^*, which is a desirable, constructive effect. However, if the two units are almost synchronized, the noise will also perturb them away from $\phi=0$, which is a destructive effect. The competition between the two effects is nonlinear. Since $\phi=0$ is an attractor with a reset, it has some degree of resistance against small levels of noise, but $\phi=\phi^*$ is a repeller and does not have this resistance. Therefore we can expect that for a range of small noise intensities and certain initial conditions, the constructive effect of noise overrides the destructive effect, which is indeed observed in Fig. 3.

A sigmoidal function was employed to represent the refractoriness (Fig. 1). However, other refractory functions can also produce similar $\delta\phi$ against ϕ curves with a repeller ϕ^*. Additional simulations indicated that the constructive effects of noise in promoting synchronization exist also with these different refractory functions.

2. Longer chains

In a chain of 30 units, an example of the evolution from random initial phases to total synchrony can be observed in Fig. 4(a). First, the units grouped into a few clusters. Then the number of clusters gradually reduced, and eventually only one big group existed. In Fig. 4(b), we can see that the presence of small levels of noise enhanced the formation and merging of clusters, and hence accelerated the overall synchronization. In the case of large levels of noise [Fig. 4(c)], the initial merging of clusters was rapid. We can see at around 3.5 time units there existed a single cluster. However, this cluster was transient and the synchronizing units split apart again due to the perturbing influence of the noise. In the case of small noise levels, however, once the system evolved to total synchrony, this pattern persisted.

The concept of a lag fixed point as discussed for the two-unit case above can also be applied to this large chain. There are $N-1$ pairs of neighbors in the system, producing $N-1$ fixed points. Each boundary of two neighboring clusters (that is, two neighboring units belonging to two different clusters) needs to be considered in turn. If these two units have a relative phase close to the lag fixed point, then they will take a long time to synchronize. Moreover, once these two units have synchronized, their neighbors may not belong to the same cluster (which means that the cluster boundary shifts). Therefore global synchronization will take a long time to achieve. In this situation, a small level of noise will perturb the units away from their particular lag fixed point, decrease their synchronization time, and help the two clusters to merge. In addition, global reorganization among clusters is also benefited from the perturbing effect of noise.

The reset mechanism, however, provides a limited resistance against noise for the synchrony attractor. If the noise level is too big, synchronized neighbors will be perturbed to nonsynchronized states. In this regime, the destructive effect of noise overrides the constructive effect.

The distribution of synchronization times, S, for different trials as shown in Fig. 5 was a tilted bell shape curve starting from $S=0$, which is the situation when the initial condition is already a total synchrony (but the probability for this to occur approaches zero). In the case of no noise [Fig. 5(a)], some very large values of S were observed. This "tail" is much shortened under optimal noise [Fig. 5(b)]. Both the mean value and the standard deviation decreased in this case. This shows that the acceleration effect was statistical (mainly through the removal of cases of long synchronization times). It becomes significant when averaged over a large number of trials of different initial conditions.

The coupling strength, w, plays a crucial role in synchronization time, S. Generally, S reduced as w increased (Fig. 7). This was to be expected since the interaction of the units are the only signal for them to organize; the stronger the interaction, the faster the process.

Figure 6 shows a plot of S vs noise intensity η. When w was weak, a distinct J-shaped curve was observed. In this situation, the system was more open to the influence of noise. S reduced rapidly for small noise levels, but also increased rapidly at larger noise levels. In contrast, when the connection strength was strong, the system was more robust against noise. The addition of noise did not cause an improvement at lower noise levels but neither did it dramatically increase S at higher levels.

Indeed, the reduction ratio Γ decreased as w increased (Fig. 8). This is also shown from the decreasing differences between the synchronization times in the absence of noise and those at optimal noise (Fig. 7), and the reduction of the definite J-shaped curves for stronger connections as evident from Fig. 6. When the connection was strong, the synchronization process was already very rapid and there was little room for further improvement. This can also be inferred from the consideration of a linked chain of two-unit systems. The change of phase difference $\delta\phi$ [Eq. (14)] depends on

coupling strength w. Numerically we can observe that the lag fixed point will become a stronger repeller (steeper slope) when the connection strength increases. The coupling plays the same role as the noise in pulling the system out of the lag fixed point. Moreover, in this regime, the system is becoming more deterministic (insensitive to noise). As a result, the acceleration effect of noise diminishes for every neighboring pair.

We can therefore identify two regimes: weak and strong coupling. The constructive effect of noise is observed in the weak connection regime only.

Figure 8 also shows that the reduction ratio (Γ) curves shift upwards as the chain length increases. Generally, the longer the chain length, the longer the synchronization time [23]. In the longer chains there is more room for improvement. A similar situation occurs in systems with weaker connections.

B. Connection noise

In our previous section, we discussed the existence of a lag region and how noise could accelerate the synchronization process by perturbing the units away from the lag fixed point. This argument appears to be also true if we implement the noise on the connection instead of the threshold. Indeed, an optimal level of noise such that the synchronization time is minimal can be seen in Fig. 9, provided that the connection is in the weak regime. As the connection strength increased, the improvement effect of noise diminished, which can be seen from the decreasing reduction ratio in Fig. 10. This is due to the increasing robustness of the system.

C. Comparison

As expected, the effect of connection noise showed a similar general trend as that of threshold noise (Figs. 11 and 12). However, their effects are not identical.

In the weak coupling regime, where J-shaped curves of S vs η are observed, the improvement effect occurred over smaller values of connection noise intensity compared to the case of threshold noise (Fig. 11). This is primarily due to the fact that the connection noise, ξ_{co}, is additive (in the form of $w+\xi_{co}$) while the threshold noise, ξ_{th}, is multiplicative.

From Eq. (4), we can see that an increase in w will increase $\frac{dV}{dt}$ such that V reaches the threshold sooner. If we keep w constant but reduce the threshold instead, the effect is similar but not identical. For example, if we reduce the threshold V_{th} from 1 to V_1 (<1), then we observe that

$$\frac{dV_i}{dt} = 1 + \sum_j w_{j\to i}\gamma_i \delta(t - t_j) \quad \text{where } V_{th} = V_1 \tag{16}$$

is equivalent to

$$\frac{dV_i}{dt} = \frac{1}{V_1} + \frac{\sum_j w_{j\to i}\gamma_i \delta(t - t_j)}{V_1} \quad \text{where } V_{th} = 1. \tag{17}$$

We notice that there is an effective increase in w (to $\frac{w}{V_1}$). By replacing V_1 with $1-\xi_{th}$, we can see that the effect of ξ_{th} is multiplicative. Comparing them,

$$w + \xi_{co} = \frac{w}{1 - \xi_{th}}, \tag{18}$$

$$\xi_{th} = \frac{\xi_{co}}{w + \xi_{co}}. \tag{19}$$

If the connection strength (which is equivalent to the size of synaptic current input in our model) plus noise is smaller than the threshold of the unit, i.e., $w+\xi_{co}<1$, then we have $\xi_{th}>\xi_{co}$ for a wide range of values. This is indeed a biologically plausible condition.

However, we also notice that in Eq. (17) there is also concurrently an increase in the intrinsic firing rate (from 1 to $\frac{1}{V_1}$). Therefore the scaling between the intensities of the two noise types is a nonlinear relationship.

For the cases of the same connection strength, the maximum time reduction in the case of threshold noise is higher than that for connection noise. This can be seen from the deeper valley in Fig. 11 and the higher reduction ratio curves in Fig. 12, as well as the distribution statistics of synchronization times. For the case of optimal connection noise in a chain of 30 units, the distribution had a mean of 37.4 with a standard deviation of 20.3 for the same number of runs, which, while still an improvement over the no noise scenario, was inferior to the optimal threshold noise case.

In the case of threshold noise, a stronger connection results in a higher robustness against noise. However, if the connection itself is noisy, the system appears to be more fragile. Moreover, a nearly linear regime in the Γ curve for weak connections was observed in the case of threshold noise but not in the connection noise, which is the result of the nonlinearity in the system.

D. Square lattice (preliminary results)

Preliminary results show that this acceleration phenomenon also occurs in the two-dimensional array (Fig. 13). In such a system, an additional way of optimization emerged. There is not only an optimal noise intensity but also an optimal connection strength such that the reduction ratio is maximal at the double optimum. This interesting phenomenon calls for future investigations.

V. CONCLUSION

In this paper, we demonstrated the phenomenon that noise accelerates the synchronization process in a chain of homogeneous oscillators. We employed the nonleaky integrate-and-fire model with a constant input and a refractory function, which may also be regarded as a biological model for pacemakers. For a range of weak connection strengths, there exists a nonzero optimal noise intensity such

that the time required for total phase synchronization is reduced. Both threshold noise and connection noise show similar effects, but they are not identical, especially in terms of scaling. In reality, it is likely that a combination of the two effects occurs.

Preliminary results on two-dimensional square lattices of these units also display the acceleration phenomenon, albeit with both an optimal noise intensity and an optimal connection strength. This leads to the hypothesis that this effect may be universal in nature.

[1] A. T. Winfree, *The Geometry of Biological Time*, 2nd ed. (Springer, New York, 2001).

[2] S. H. Strogatz, *Sync: The Emerging Science of Spontaneous Order* (Hyperion, New York, 2003).

[3] Y. Kuramoto, in *International Symposium on Mathematical Problems in Theoretical Physics*, edited by H. Araki, Lectures Notes in Physics No. 30 (Springer, New York, 1975), p. 420.

[4] J. A. Acebron, L. L. Bonilla, C. J. P. Vicente, F. Ritort, and R. Spigler, Rev. Mod. Phys. **77**, 137 (2005).

[5] D. Golomb, D. Hansel, B. Shraiman, and H. Sompolinsky, Phys. Rev. A **45**, 3516 (1992).

[6] K. Okuda, Physica D **63**, 424 (1993).

[7] D. Hansel, G. Mato, and C. Meunier, Phys. Rev. E **48**, 3470 (1993).

[8] L. L. Bonilla, C. J. Perez Vicente, F. Ritort, and J. Soler, Phys. Rev. Lett. **81**, 3643 (1998).

[9] L. F. Abbott, Brain Res. Bull. **50**, 303 (1999).

[10] A. H. Cohen, P. J. Holmes, and R. H. Rand, J. Math. Biol. **13**, 345 (1982).

[11] R. E. Mirollo and S. H. Strogatz, SIAM J. Appl. Math. **50**, 1645 (1990).

[12] X. Guardiola, A. Diaz-Guilera, M. Llas, and C. J. Perez, Phys. Rev. E **62**, 5565 (2000).

[13] P. C. Bressloff and S. Coombes, Neural Comput. **12**, 91 (2000).

[14] B. Lindner, J. Garcia-Ojalvo, A. Neiman, and L. Schimansky-Geier, Phys. Rep. **392**, 321 (2004).

[15] T. Turova, W. Mommaerts, and C. van der Menlen, Stochastic Proc. Appl. **50**, 173 (1994).

[16] J. Pham, K. Pakdaman, and J.-F. Vibert, BioSystems **48**, 179 (1998).

[17] P. H. E. Tiesinga and J. V. Jose, J. Comput. Neurosci. **9**, 49 (2000).

[18] Y. Wang, D. T. W. Chik, and Z. D. Wang, Phys. Rev. E **61**, 740 (2000).

[19] B. Hu and C. Zhou, Phys. Rev. E **61**, R1001 (2000).

[20] K. Pakdaman and D. Mestivier, Physica D **192**, 123 (2004).

[21] D. S. Goldobin and A. Pikovsky, Phys. Rev. E **71**, 045201(R) (2005).

[22] S. Guan, Y.-C. Lai, C.-H. Lai, and X. Gong, Phys. Lett. A **353**, 30 (2006).

[23] S. R. Campbell, D. L. Wang, and C. Jayaprakash, IEEE Trans. Neural Netw. **15**, 1027 (2004).

[24] P. V. E. McClintock and F. Moss, in *Noise in Nonlinear Dynamical Systems*, edited by F. Moss and P. V. E. McClintock (Cambridge University Press, Cambridge, England, 1989), Vol. 3, p. 243.

[25] W. Gerstner and W. M. Kistler, *Spiking Neuron Models. Single Neurons, Populations, Plasticity* (Cambridge University Press, Cambridge, England, 2002), Chap. 5.

[26] J. A. White, J. T. Rubinstein, and A. R. Kay, Trends Neurosci. **23**, 131 (2000).

[27] A. Manwani and C. Koch, Neural Comput. **11**, 1797 (1999).